Colloquium: Random matrices and chaos in nuclear spectra

T. Papenbrock

Department of Physics and Astronomy, University of Tennessee,
Knoxville, Tennessee 37996, USA
and Physics Division, Oak Ridge National Laboratory, Oak Ridge, Tennessee 37831, USA

H. A. Weidenmüller

Max-Planck-Institut für Kernphysik, D-69029 Heidelberg, Germany

(Published 8 August 2007)

Chaos occurs in quantum systems if the statistical properties of the eigenvalue spectrum coincide with predictions of random-matrix theory. Chaos is a typical feature of atomic nuclei and other self-bound Fermi systems. How can the existence of chaos be reconciled with the known dynamical features of spherical nuclei? Such nuclei are described by the shell model (a mean-field theory) plus a residual interaction. The question is answered using a statistical approach (the two-body random ensemble): The matrix elements of the residual interaction are taken to be random variables. Chaos is shown to be a generic feature of the ensemble and some of its properties are displayed, emphasizing those which differ from standard random-matrix theory. In particular, the existence of correlations among spectra carrying different quantum numbers is demonstrated. These are subject to experimental verification.

PACS number(s): 21.60.Cs, 24.60.Lz, 21.10.Hw, 24.60.Ky

CONTENTS

I. RANDOM MATRICES AND CHAOS

A. Introduction

This Colloquium presents the application of random matrices to nuclear spectroscopy. We discuss the origin of random-matrix theory (RMT), some of its predictions, and its relation to classical chaos. We show that the predictions of RMT often agree well with spectroscopic data in nuclei. In the main part of the paper, we address the question: How can this success of RMT be reconciled with our knowledge of the dynamical behavior of nuclei as embodied in the nuclear shell model? Although actually formulated for nuclei, our arguments apply likewise in modified form to other Fermi systems like atoms and molecules.

Near the ground state, the spectra of self-bound Fermi systems are essentially discrete. As an example, Fig. 1 shows the measured spectrum of the nucleus ^{19}O. Up to the threshold for decay into a neutron (n) and ^{18}O (the neutron threshold) at an excitation energy of 3.957 MeV, the levels shown decay only by gamma emission; the ground state is unstable against beta decay. The long lifetimes of these decay modes render the levels virtually discrete. Above the neutron threshold, the levels acquire finite particle decay widths (which typically are much larger than those for beta and gamma decay) and are also seen as resonances in cross sections (similar to the ones in the reaction $n + {}^{18}$O). The levels in Fig. 1 carry quantum numbers which reflect symmetries of the nuclear Hamiltonian: Total spin J corresponds to rotational invariance, total isospin T to proton-neutron symmetry, and parity P to mirror reflection symmetry. In heavy nuclei, because of the Coulomb interaction between protons the isospin is no longer a good quantum number. In its general appearance, Fig. 1 is representative not only for nuclei but also for atoms, molecules, and atomic clusters.

B. Regular motion

The excitation energies and widths for beta, gamma, and particle decay of the levels found experimentally can often be described in terms of simple integrable dynamical models. In analogy to classical mechanics, we
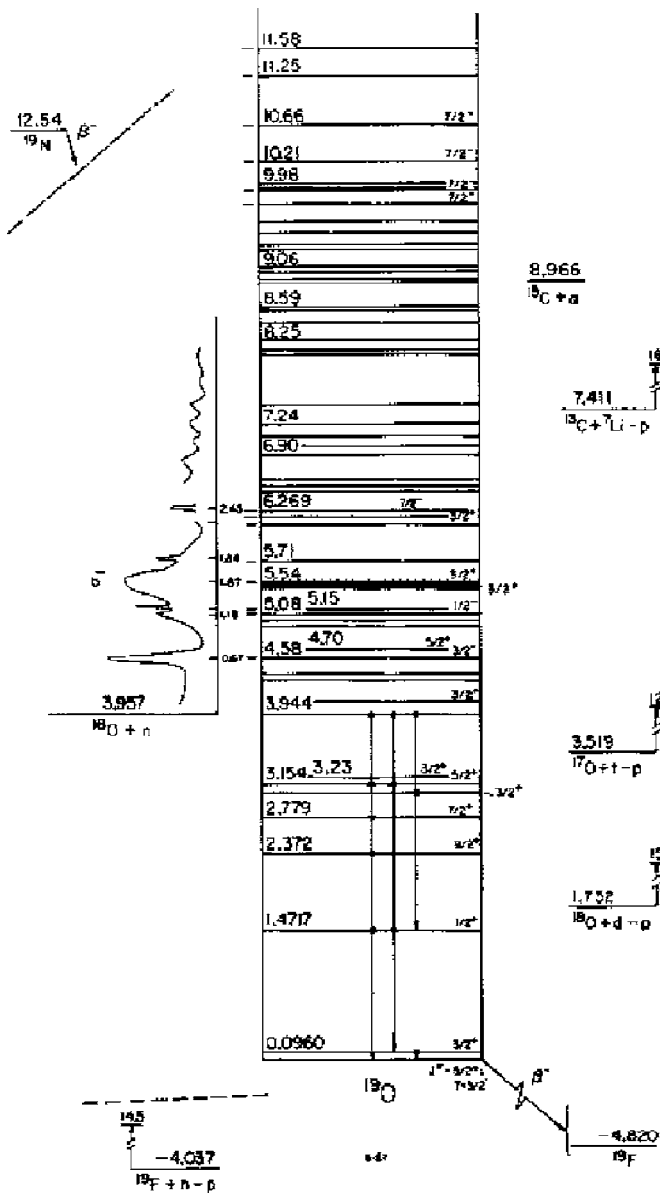
FIG. 1. The spectrum of ^{19}O. From Ajzenberg-Selove, 1987.

FIG. 2. Rotational bands in ^{174}Hf. From Bohr and Mottelson, 1975.

then speak of regular motion. A striking example is furnished by the existence of rotational bands. These are characterized by a spin-parity J^P sequence $0^+, 2^+, 4^+, \ldots$ and excitation energies proportional to $J(J+1)$. They correspond to a rotation of the entire (nonspherical) nucleus about some axis. Figure 2 shows two such bands in the nucleus ^{174}Hf. Another example for regular motion is provided by the independent-particle model: nucleons move independently in the mean field of the nucleus. This model corresponds to the most elementary version of the nuclear shell model and accounts for the existence of "magic numbers" for neutrons and protons (i.e., numbers where a major shell is filled and where the nuclear binding energy attains maxima) as well as for spins and parities of ground states of nuclei differing by one unit in proton or neutron number from closed-shell nuclei. We discuss the nuclear shell model in the next section.
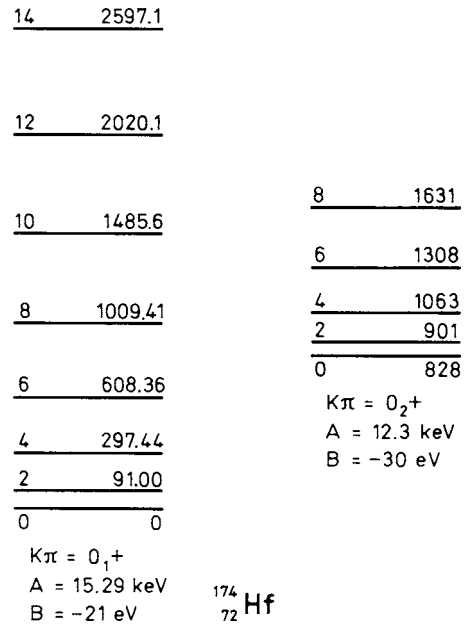
C. Nonregular motion

The emphasis in this paper is on chaotic motion in nuclei. The previous subsection serves as a reminder that there is strong evidence for regular motion in nuclei, especially in the vicinity of the ground state. We now turn to the equally strong evidence for chaotic motion. We first present a semihistorical narrative.

The first evidence for chaotic motion in nuclei came from spectroscopic data on levels at neutron threshold, i.e., rather far from the ground state. In general, it is exceedingly difficult to unambiguously identify the positions, spins, and parities of such levels. Neutron time-of-flight spectroscopy offers the unique opportunity to acquire precise spectroscopic information in a range of excitation energies which is otherwise virtually inaccessible. The neutron threshold in medium-mass and heavy nuclei typically occurs at an excitation energy of 5–7 MeV (and not at ≈ 4 MeV as in ^{19}O; see Fig. 1). Measuring the total cross section for slow neutrons versus kinetic energy, one observes resonances. Each of the resonances corresponds to a nuclear state at an excitation energy of around 5 or 7 MeV. The ground states of even-even nuclei have spin-parity 0^+. Slow neutrons carry angular momentum 0 and have spin 1/2. For even-even target nuclei, the states seen, therefore, all have spin-parity $1/2^+$. We show here not the earliest but some of the best data. In the 1970s, the Columbia group measured time-of-flight spectra of slow neutrons scattered on a number of heavy nuclei. For each target nucleus, they observed a sequence of up to 200 $1/2^+$ levels. (That number was limited by the resolution of the time-of-flight spectrometer.) Figure 3 shows their data for the total neutron scattering cross section on ^{238}U versus neutron energy. We see a number of very narrow resonances (widths typically smaller than 1 eV) with typical spacings

FIG. 3. Total cross section for scattering of neutrons by ^{238}U vs neutron energy. The abscissa spans about 80 eV in each of the four plots. From Garg *et al.*, 1964.

of 10 eV. The energies of the associated levels were determined with the help of an *R*-matrix multilevel analysis (Lane and Thomas, 1958).

Already in the 1930s, similar data (of much inferior quality) had led Bohr to formulate his compound-nucleus hypothesis (Bohr, 1936). Bohr argued that the existence of narrowly spaced narrow resonances is incompatible with independent-particle motion in the nucleus. Indeed, simple estimates using a central potential yield single-particle *s*-wave level spacings around 1 MeV (and not 10 eV as shown in Fig. 3) and *s*-wave decay widths for neutron-instable states of around 100 keV (and not <1 eV as shown in Fig. 3). Bohr argued that the existence of such narrow resonances could not be understood without assuming strong interactions between the incident neutron and the nucleons in the target. A wooden toy model (shown in Fig. 4) was used to demonstrate this idea of the compound nucleus. The billiard balls represent nucleons, the queue indicates the kinetic energy of the incident neutron, and the trough simulates the attractive mean field. Since the publication of Bohr's 1936 paper and until the discovery of the nuclear shell model in 1949, the idea of independent-particle motion in the nucleus was virtually unacceptable in the nuclear physics community. And as we shall see, understanding chaos in nuclei is almost synonymous to

reconciling Bohr's idea of the compound nucleus with the nuclear shell model.

D. Random matrices

When Wigner (1955) introduced random matrices into physics, he did not refer explicitly to Bohr (1936). Nevertheless, we believe that his work was motivated by and can be seen as the mathematical formulation of the idea of the compound nucleus. It is noteworthy that the work started in 1951, two years after the discovery of the shell model.

How can one deal with a situation where the constituents of a quantum system strongly interact? Suppose that we are dealing with a nonintegrable system without
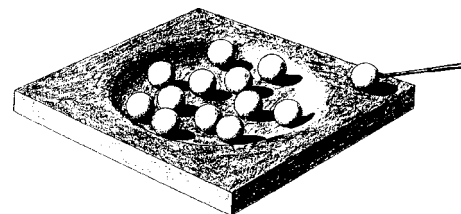

FIG. 4. Wooden toy model simulating Bohr's compound nucleus. Ref.: Nature **137**, 351 (1936).

remaining symmetries. By that we mean that extant symmetries of the Hamiltonian like total spin and parity have been taken into account; the Hamiltonian has block-diagonal form; the individual blocks are free of further symmetries. We focus attention on one such block to which we refer for simplicity as the Hamiltonian. Is it possible to make generic statements about the spectrum and eigenvalues of such a system? Following Wigner (1959), we consider the matrix representation $H_{\mu\nu}$ of the Hamiltonian in Hilbert space. Here $\mu, \nu = 1, \ldots, N$ and $N \gg 1$ (we let $N \rightarrow \infty$ at the end of the calculation). Nuclei are time-reversal invariant. Therefore, we can choose a representation where $H_{\mu\nu}$ is real and symmetric. There are no further symmetries beyond rotational symmetry and parity. Now comes the decisive and unusual step: Rather than considering the individual Hamiltonian of the actual physical system, we study an entire ensemble of Hamiltonians, all having the same symmetry. It turns out that while we cannot make generic statements about the individual Hamiltonian, such statements are possible about almost all members of the ensemble.

The ensemble is defined in such a way that it combines generality with the symmetry of H: It consists of real and symmetric matrices. To avoid a preferred direction in Hilbert space, it is chosen to be invariant under those transformations in Hilbert space which preserve the symmetry of H. These are the orthogonal transformations. The ensemble is defined in terms of a probability density in matrix space. The probability density has the form

$$C \exp\left(-\frac{N \operatorname{tr}(H^2)}{\lambda^2}\right) \prod_{\mu \leq \nu} dH_{\mu\nu}. \tag{1}$$

The last factor is the product of the differentials of the independent matrix elements. This factor is orthogonally invariant and so is the trace of H^2 in the exponent. The Gaussian factor is introduced because a cutoff is needed to render the integrals over matrix space convergent. The ensemble is characterized by a single parameter λ, which has the dimension of energy. This parameter determines the mean level spacing of the ensemble, i.e., the mean value of the distance between two neighboring eigenvalues. We are interested in the *fluctuations* of the spacings of neighboring levels around that mean value and in the correlations between spacings of different pairs of neighboring levels. These are characterized by certain local fluctuation measures which are introduced below. All measures depend on the level spacing expressed in units of the mean level spacing and are, therefore, independent of the parameter λ and altogether parameter free. The factor C is a normalization factor. The factor N in the exponent (with N the matrix dimension) guarantees that the spectrum has finite range. Equation (1) defines the Gaussian orthogonal ensemble (GOE) of random matrices. Dyson (1962a, 1962b, 1962c) showed that there are three canonical random-matrix ensembles defined by symmetry: the GOE, the Gaussian unitary ensemble (GUE) (for time-reversal noninvariant systems), and the Gaussian symplectic ensemble (GSE) (for
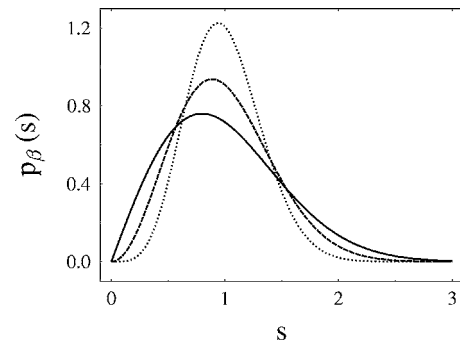

FIG. 5. The nearest-neighbor spacing distribution $P_\beta(s)$ vs s, the actual spacing in units of the mean level spacing, for the three canonical ensembles with $\beta = 1$, 2, and 4 (solid, dashed, and dotted lines, respectively). $\beta = 2$ corresponds to the GOE. From Guhr *et al.*, 1998.

systems with half-integer spin which are not rotationally invariant). The ensembles GUE, GOE, and GSE carry the Dyson parameters $\beta = 1$, 2, and 4, respectively.

While the symmetry of the Hamiltonian and thus the form of the invariant measure in expression (1) is dictated by quantum mechanics, the choice of the Gaussian cutoff is arbitrary and dictated by convenience. It has been shown, however, that an entire class of different choices (like, for instance, taking the trace of the fourth power of H in the exponent) yields the same results for the local fluctuation measures. This important property is referred to as universality of the ensemble. It guarantees that the local fluctuation measures predicted by the GOE are generic.

Random-matrix theory (RMT) only predicts ensemble averages of observables [calculated by integrating the observable over the ensemble (1)]. But experimentally we deal with a single Hamiltonian, not an ensemble. The applicability of RMT to a single system is guaranteed by the property of ergodicity: For almost all members of the ensemble, the ensemble average of an observable (as given by RMT) is equal to the running average of that observable over the spectrum of a single member. Ergodicity guarantees that the quantitative and parameter-free predictions of RMT can be meaningfully compared with experimental data.

E. Fluctuation measures

The two fluctuation measures most frequently employed in analyzing data are the nearest-neighbor spacing (NNS) distribution and the Dyson-Mehta (Mehta, 2004) or Δ_3 statistic. Figure 5 gives the NNS distribution $P_\beta(s)$, i.e., the probability distribution of spacings, versus s (the actual spacing of two neighboring eigenvalues in units of their mean spacing) for Dyson's three canonical ensembles. The distributions are characterized by level repulsion at short distances [$P_\beta(s) \propto s^\beta$ for small s] and a Gaussian falloff for large s. We note that if the system were integrable, all eigenvalues would carry different quantum numbers and level repulsion would be absent. The Δ_3 statistic measures correlations between eigen-

value spacings. Let $\mathcal{N}(E)$ denote the total number of levels below energy E. Clearly $\mathcal{N}(E)$ is a step function which increases by one unit as E passes an eigenvalue. The Δ_3 statistic measures how well $\mathcal{N}(E)$ is on average approximated by a straight line. The statistic is defined by

$$\Delta_3(L) = \left\langle \min_{a,b} \frac{1}{L} \int_{E_0}^{E_0+L} (\mathcal{N}(E') - aE' - b)^2 dE' \right\rangle_{E_0}.$$
(2)

Minimization with respect to a and b determines the best straight line. The angular brackets denote an average over the initial energy E_0 and over the ensemble. All energies are in units of the mean level spacing, and $\Delta_3(L)$ is, therefore, parameter free. If the spacings were totally uncorrelated, then Δ_3 would be linear in L. It would grow much slower with L if the spacings were correlated in such a way that a large spacing is always followed by a small one and vice versa. The actual behavior of $\Delta_3(L)$ is shown as a solid line in Fig. 7: $\Delta_3(L)$ grows essentially logarithmically with L. This property is referred to as the stiffness of RMT spectra.

It is important to note, for later discussion that a GOE spectrum does not carry any information content beyond the mean level spacing. This is obvious since any realization of H is obtained by drawing random numbers from the Gaussian distribution (1). Thus, it would not be worthwhile to apply spectroscopic analyses to such a spectrum. Put differently, a GOE Hamiltonian has $N(N+1)/2$ independent matrix elements. Counting shows that we need to measure all N eigenvalues and all N eigenfunctions to reconstruct H. This is very different for typical dynamical systems where the Hamiltonian is known except for a small number of parameters.

F. Quantum chaos

Suppose the fluctuation measures of an experimental spectrum agree with GOE predictions. What does such a result imply physically? The answer to this question was better understood with the study of few-degrees-of-freedom quantum systems which are chaotic in the classical limit. The development culminated in the Bohigas-Giannoni-Schmit conjecture (Bohigas *et al.*, 1986). It says that *the spectral fluctuation properties of a quantum system which is chaotic in the classical limit coincide with those of the canonical random-matrix ensemble that has the same symmetry*. Bohigas *et al.* (1986) supported their conjecture by calculating numerically the NNS distribution and the Δ_3 statistic for the Sinai billiard, a system which is time-reversal invariant and fully chaotic in the classical limit, and comparing the result with the GOE prediction. This is shown in Figs. 6 and 7.

Agreement like the one shown in Figs. 6 and 7 has since been found in many other chaotic systems. Moreover, an analytical proof of the Bohigas-Giannoni-Schmit conjecture has recently been published (Heusler *et al.*, 2007). That proof uses the semiclassical approxi-
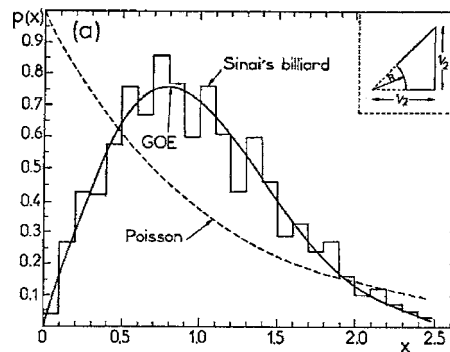

FIG. 6. The NNS distribution for the Sinai billiard (histogram) and the GOE prediction (solid line). From Bohigas *et al.*, 1986.

mation and generic properties of chaotic trajectories. We are thus led to consider agreement between the spectral fluctuations of a physical system and RMT predictions as a signal for chaotic motion. It is in that sense that we use the word chaos also in nuclei. This is done with a caveat: The semiclassical proof by Heusler *et al.* (2007) is not applicable directly to nuclei because nuclei are too dense to admit a semiclassical approximation.

Quantum chaos has been studied intensely during the last 20 years or so (Haake, 2001). These studies have focused mainly on dynamical systems with few degrees of freedom. The Sinai billiard is a prime example. Here chaos is due to the fact that the inner circle and the outer rectangle possess incommensurate symmetries. In contradistinction, the atomic nucleus is a many-body system. We show that in such a system the dynamical features which cause chaos are distinctly different from the ones which cause chaos in few-degrees-of-freedom systems.

G. Chaos in nuclei

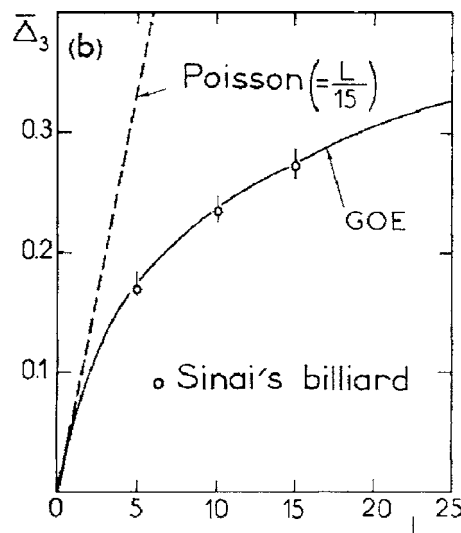We are now in the position to return to the data shown in Fig. 3. Combining the information on the ex-

FIG. 7. The Δ_3 for the Sinai billiard (histogram) and the GOE prediction (solid line). From Bohigas *et al.*, 1986.
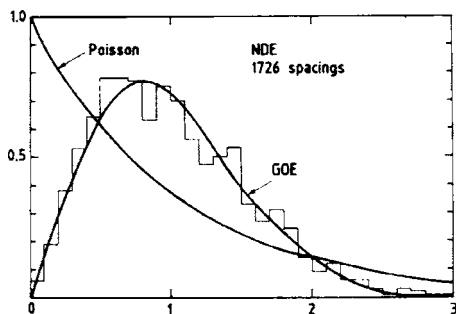
FIG. 8. The NNS distribution for the nuclear data ensemble (histogram) and the GOE prediction (solid line). From Haq *et al.*, 1983.

cited levels in ^{239}U obtained from these data with that of many similar experiments on the scattering of slow neutrons and of protons at the Coulomb barrier by other nuclei, Haq *et al.* (1982, 1983) formed the nuclear data ensemble. It consists of 1726 spacings. These were used to determine the NNS distribution and the Δ_3 statistic. The results are shown in Figs. 8 and 9. The solid lines labeled Poisson correspond to totally uncorrelated levels and thus to integrable systems. The agreement with the GOE prediction is impressive. We conclude that at neutron threshold (and at the Coulomb barrier for protons) nuclei display chaotic motion. The deep physical insight of N. Bohr, who conceived the compound nucleus idea and designed the toy model of Fig. 4, is borne out by the data: Idealized models of billiards are prime examples of chaotic motion, and nuclear levels at neutron threshold display chaotic behavior. Since 1983, there has also been growing evidence for chaotic motion in nuclei at lower excitation energies, although the statistics of such data is usually not as good as near the neutron threshold.

In conclusion, there is strong evidence for chaotic motion in nuclei. How can this evidence be reconciled with the extant information on nuclear dynamics (the shell model)? And—given the fact that GOE spectra carry zero information content beyond the mean level spacing—which is the information content of nuclear spectra in the regime of chaotic motion? These are the
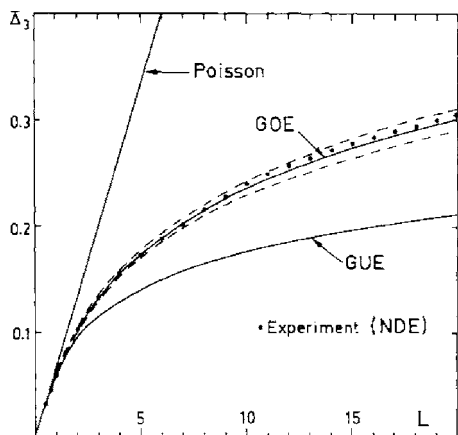

FIG. 9. The Δ_3 for the nuclear data ensemble (data points) and the GOE prediction (solid line). From Haq *et al.*, 1982.
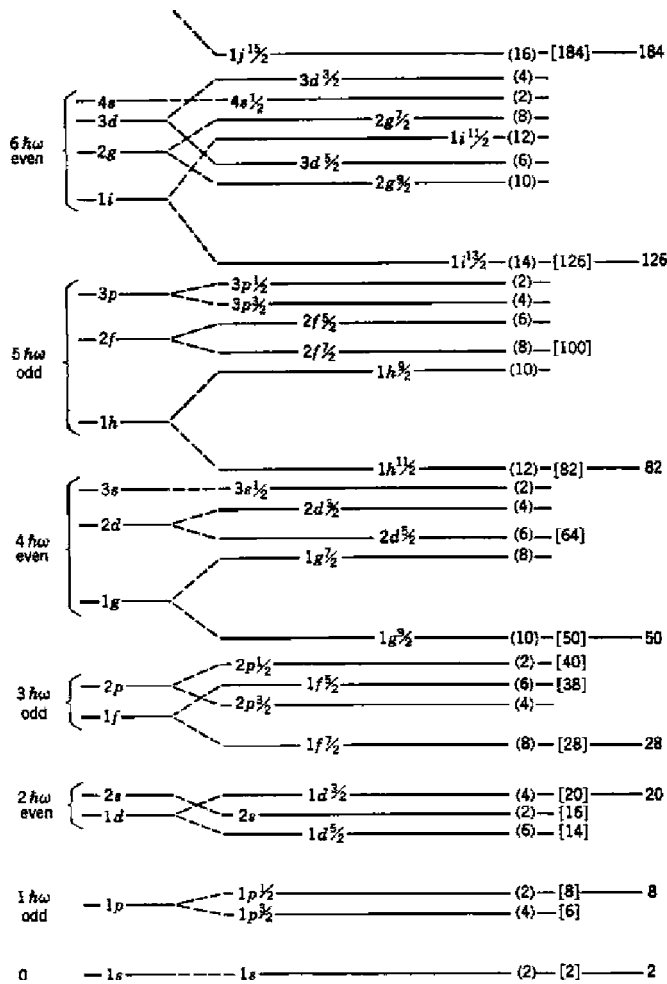

FIG. 10. Level sequence in the nuclear shell model. The orbitals are labeled by their spectroscopic notation, and the number of available single-particle states is shown. From Mayer and Jensen, 1955.

questions we address in the remainder of this paper.

II. DYNAMICAL ASPECTS

A. Chaos in the nuclear shell model

The shell model is the universal model for the structure of atoms and nuclei. In nuclei, it consists of a central potential U with a strong spin-orbit interaction (the mean field) and a fairly weak residual interaction V which accounts for the remaining part of the nucleon-nucleon interaction. The central potential U defines the major shells shown in Fig. 10: The $1s$ shell, the $1p$ shell, the $2s1d$ shell, etc., in spectroscopic notation, the latter with the subshells $s_{1/2}$, $d_{3/2}$, and $d_{5/2}$ where the indices denote the nucleon spin. The subshells have different single-particle energies, and the states within a major shell are, therefore, not totally degenerate. Still, large degeneracies remain when the shell contains more than a single nucleon. These degeneracies are lifted by the residual interaction V. That interaction conserves parity and is rotationally invariant and invariant under time

reversal. It is weak in the sense that it produces configuration mixing primarily within the same major shell. More precisely, the magnitude of a typical matrix element is small compared with the spacing of the centroids of adjacent major shells but comparable with that of adjacent subshells in the same major shell. In all that follows we, therefore, consider only a single major shell. And the residual interaction is predominantly a two-body interaction, $V = \Sigma_{\alpha < \beta} V(\vec{r}_\alpha, \vec{r}_\beta)$, although there is evidence that three-body forces are needed to obtain quantitative agreement with experimental spectra. Again, we confine ourselves for simplicity to two-body forces.

The Hamiltonian of the shell model is

$$H = \sum_\alpha \left(-\frac{\hbar^2}{2m}\Delta_\alpha + U(\vec{r}_\alpha) \right) + \sum_{\alpha < \beta} V(\vec{r}_\alpha, \vec{r}_\beta). \tag{3}$$

Here $\vec{r}_\alpha$ denotes the coordinates and spin-isospin degrees of freedom of the nucleon labeled α. The single-particle part of H has eigenstates $|j\rangle$ and eigenvalues ε_j. We use second quantization and write H as

$$H = \sum_j \varepsilon_j a_j^\dagger a_j + \frac{1}{4}\sum_{ijkl} v(ij;kl)a_i^\dagger a_j^\dagger a_l a_k. \tag{4}$$

Here $a_j^\dagger$ creates a nucleon in a single-particle state j. The two-body matrix elements $v(ij;kl)$ represent the residual interaction. In writing Eq. (4) we have not paid attention to conserved quantum numbers like spin and isospin. This was done in order to keep the notation simple. More details are given in Sec. II.B.

In the shell model it is assumed that all shells but one are completely filled and attention is focused on that last shell (the valence shell). Distributing the valence nucleons over the various subshells in the valence shell, one constructs a basis of antisymmetrized many-body states $|J\mu\rangle$. We use a shorthand notation where J stands for total spin, total isospin, and parity, while μ is a running index. These are used to calculate the matrix elements

$$H_{\mu\nu}(J) = \langle J\mu|H|J\nu\rangle \tag{5}$$

of the Hamiltonian (4) in the subspace with quantum numbers J. Diagonalization of $H_{\mu\nu}(J)$ yields the eigenvalues and eigenfunctions. The latter are used to calculate various transition matrix elements. This scheme has been used with considerable success in many parts of the periodic table. Exceptions are mainly deformed nuclei which occur in the middle between large major shells. When we refer to Eq. (4) in the text further below, we always do so with the understanding that that equation refers to the valence shell only.

In the following we focus attention on the $2s1d$ shell (in short, the sd shell). The $1s$ shell and the $1p$ shell are filled, taking a total of 16 nucleons. Thus, the sd shell describes nuclei with mass numbers between 16 (O) and 40 (Ca). We do so for practical reasons: The dimensions of the Hamiltonian matrices in the sd shell are quite manageable (maximal dimensions are of the order of 10^3) while much larger numbers occur in higher shells. We sometimes consider also a single j shell with half-
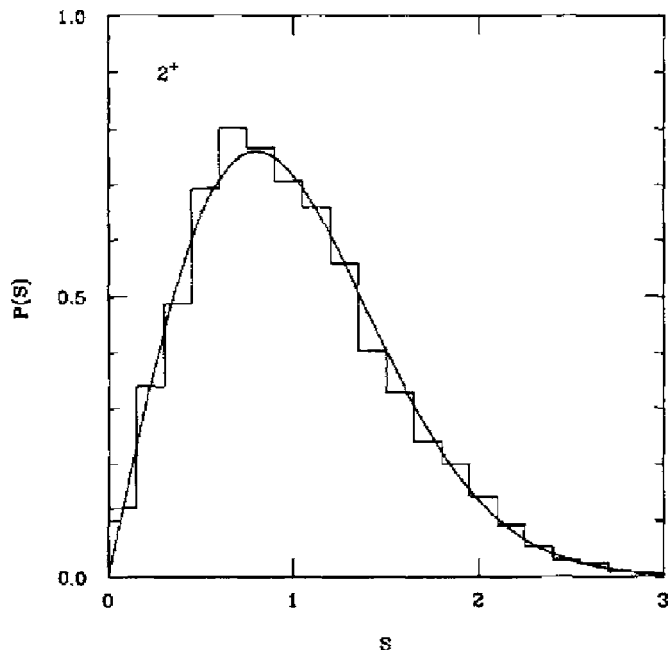

FIG. 11. The NNS spacing distribution for the $J=2$, $T=0$ states of 12 nucleons in the sd shell (histogram) compared to the GOE (line). From Zelevinsky *et al.*, 1996.

integer j. Although not realistic in the framework of the nuclear shell model, this idealization is useful for purposes of orientation.

Which are the fluctuation properties of the resulting spectra? That question was studied, for instance, by Zelevinsky *et al.* (1996). The authors used standard single-particle energies and a standard two-body residual interaction to calculate the positions of the states with spin $J=2$ and isospin $T=0$ for 12 nucleons in the sd shell. The matrix dimension is 874. In Figs. 11 and 12, the NNS spacing distribution and the Δ_3 statistic for these levels are compared with GOE predictions. The agreement is very good. (It would be desirable to confirm this result experimentally. Unfortunately, the data needed are not available: There are no more than a handful of levels known for each value of spin and isospin; such levels cluster in the vicinity of the ground state.) Zelevinsky *et al.* (1996) described numerous further results (on thermodynamic properties, on the statistics of eigenfunctions, etc.). While it was found that the input used in shell-model calculations (the distribution of many-body matrix elements) differs from that used in the GOE, the results agree to a very large extent with GOE predictions.

The result displayed in Figs. 11 and 12 and other results obtained on chaos in shell-model calculations are surprising and call for a deeper analysis. Indeed, the Hamiltonian of the shell model is quite different from a GOE matrix. And yet, it is able to produce GOE-like spectral fluctuations. It does not seem unreasonable to speculate that the shell model would also be able to account for the GOE-like spectral fluctuations shown in Figs. 8 and 9 (this cannot be checked because of the large dimensions of the matrices involved). At the same
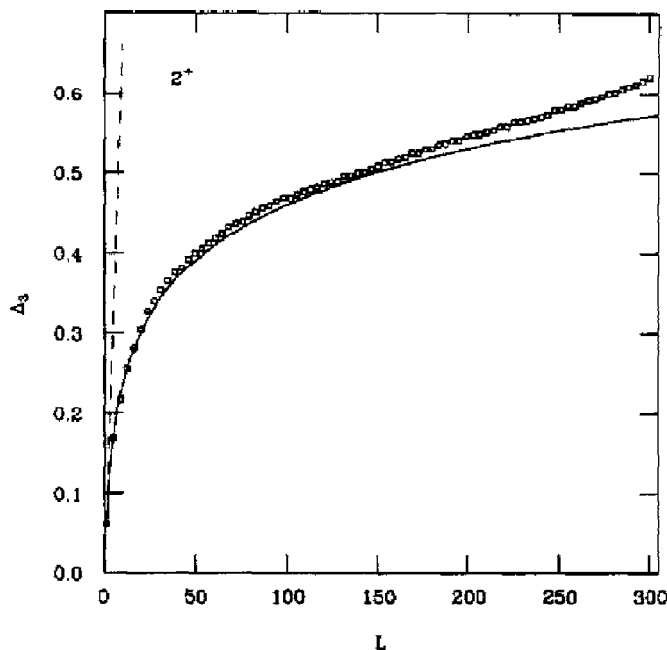
FIG. 12. The Δ_3 statistic for the $J=2$, $T=0$ states of 12 nucleons in the *sd* shell (data points) compared to the GOE (solid line). From Zelevinsky *et al.*, 1996.

time, the shell model accounts well for some regular features observed experimentally like magic numbers and spectroscopic data on low-lying states. The questions raised at the end of Sec. I.G must, therefore, be reformulated as follows: Are the results shown in Figs. 11 and 12 a generic property of the shell model or are they due to very special circumstances? In other words: How is chaos produced in the shell model? And what is the information content of shell-model spectra? A further question would be: How does the shell model manage to produce both regularity and chaos? We will not address that last question. Suffice it to say that regularity is mostly seen when considering states with different quantum numbers like in Fig. 2, while chaos is manifest in long sequences of states carrying identical quantum numbers. The way we use them here, regularity and chaos are not necessarily contradictory concepts.

B. Two-body random ensemble

To answer these questions, it is necessary to go somewhat more deeply into the details of shell-model calculations. The single-particle states in the shell model carry the half-integer spin quantum number j. The two-body interaction scatters a pair of nucleons in states (j_1, j_2) into states (j_3, j_4) which may or may not be identical to (j_1, j_2). The two-body interaction conserves total spin, total isospin, and parity. Coupling the initial and final pairs of states to total spin s (and suppressing the analogous coupling for isospin for simplicity), we write the antisymmetrized reduced matrix elements of the two-body interaction in the form $\langle j_3 j_4 s | V | j_1 j_2 s \rangle$ or more simply as $v(\alpha)$ where the index α labels different two-body matrix ele-

ments. (The word "different" refers to matrix elements not connected by symmetry properties.) Counting (which must include spin and isospin) shows that in the *sd* shell, α ranges from 1 to 63 and, in a single j shell with half-integer j, from 1 to $j+1/2$.

Chaos has to do with the complete mixing of states in Hilbert space. How does the residual interaction accomplish such mixing? We focus attention on the two-body interaction and assume that all subshells belonging to a major shell are degenerate. [It is intuitively obvious and has been shown numerically that the mixing of shell-model states becomes weaker as the differences between single-particle energies of subshells become comparable to the magnitudes of the $v(\alpha)$.] We accordingly omit the single-particle energies in Eq. (4) altogether. The Hamiltonian $H_{\mu\nu}$ of Eq. (5) is then completely determined by the two-body interaction in Eq. (4). Thus, it has the form

$$H_{\mu\nu}(J) = \sum_\alpha v(\alpha) C_{\mu\nu}(J, \alpha). \tag{6}$$

The sum over α is equivalent to the sum over $\{ijkl\}$ in Eq. (4). Each term in the sum in Eq. (6) is the product of two contributions. The $v(\alpha)$ stand for the matrix elements denoted by $v(ij; kl)$ in Eq. (4) (except that we have now paid proper attention to the coupling of angular momenta) and represent the specific features of the two-body interaction. Except for angular momentum coupling coefficients, the elements of the coefficient matrices $C_{\mu\nu}(J, \alpha)$ are the matrix elements of the operators $a_i^\dagger a_j^\dagger a_l a_k$ in Eq. (4). These matrices are determined by the major shell we are in, by the coupling scheme we have chosen to construct the states $|J\mu\rangle$, and by the specific two-body interaction operator labeled α which defines the matrix element $v(\alpha)$. The matrices $C_{\mu\nu}(J, \alpha)$ represent the geometry and symmetries of the shell model and are generic in the sense that they are independent of the actual choice of the residual interaction. The seemingly trivial equation (6) actually contains very useful information about chaos in the shell model.

To answer the question how the residual interaction causes chaos in the most general terms, we study the Hamiltonian (6) for the most general two-body interaction. This is accomplished by assuming that the elements $v(\alpha)$ of the two-body interaction are Gaussian-distributed random variables with mean value zero and a common second moment. The value of the second moment is irrelevant since it determines only the overall scale of the spectrum. With this assumption, the matrices (6) form an ensemble of Gaussian-distributed random matrices. This two-body random ensemble (TBRE) of the shell model was originally introduced in the 1970s by French and Wong (1970) and by Bohigas and Flores (1971). The TBRE is tailored to the shell model and, therefore, much more realistic than the GOE. The ensemble being defined in terms of an integration over the Gaussian variables $v(\alpha)$, statements derived by averaging over the ensemble hold for all members of the ensemble with the exception of a set of measure zero with respect to that integration measure.

Within the TBRE, $v(\alpha)$ play a minor role only: They determine the specific linear combination of the matrices $C_{\mu\nu}(J,\alpha)$ which forms the Hamiltonian. If the Hamiltonian causes chaos for almost all choices of $v(\alpha)$, this property must be inherent in the matrices $C_{\mu\nu}(J,\alpha)$. Therefore, an analytic theory has to address these matrices as the fundamental building blocks of the TBRE. Unfortunately, such a theory is in its infancy as yet. An analytically more accesible ensemble is provided by the embedded Gaussian orthogonal ensemble EGOE(k) (Mon and French, 1975). This ensemble is defined as a random-matrix ensemble of m fermions occupying l degenerate single-particle levels with Gaussian-distributed random k-body interaction matrix elements, but assumes no further symmetries like spin and isospin. For $k=m$, the EGOE(k) becomes the GOE, and for $k=2$, it becomes the analog of the TBRE without quantum numbers. For recent reviews, we refer the reader to Kota (2001) and Benet and Weidenmüller (2003). Less is known for the TBRE. In the following, we describe some insights that have been gained over the last few years.

C. Comparison of GOE and TBRE

The GOE has three important properties: It is invariant under orthogonal transformations (hence, analytically tractable), it is universal, and it is ergodic. The TBRE probably does not share any of these properties. The set of matrices $C_{\mu\nu}(J,\alpha)$ is fixed. A unitary transformation of all matrices generates another representation of the ensemble but not another member of the ensemble. Therefore, the TBRE is not unitarily invariant. It is not clear how a non-Gaussian distribution of $v(\alpha)$ would affect spectral fluctuation properties of the TBRE. In the case of the GOE, local fluctuation properties and global spectral properties become separated in the limit $N \to \infty$. This separation is at the root of universality (local fluctuation properties do not depend on the form of the distribution of the matrix elements). By definition, the TBRE is linked to a specific shell; its matrices have finite dimension. Similarly for ergodicity: For the GOE, this is proved by showing that correlation functions vanish with increasing distance of their energy arguments. The proof uses the limit $N \to \infty$. This limit does not exist in the TBRE. One is tempted to ask: Why bother with the TBRE? The answer is: The TBRE is more realistic than the GOE. Moreover, it might be possible to study the TBRE analytically for the case of a single j shell and to prove universality and ergodicity in the limit $j \to \infty$.

Except for mirror symmetry about the main digonal, every element of a GOE Hamiltonian matrix stands for an independent random variable. For $N \gg 1$, the number $N(N+1)/2$ of such variables is much larger than the matrix dimension N. The number n of independent random variables in the TBRE is typically small in comparison with the matrix dimension. For the case of a single j shell, n grows linearly with j while the typical matrix

dimension grows exponentially with j. In the GOE, the analogs of the matrices $C_{\mu\nu}(J,\alpha)$ exist. These are the $N(N+1)/2$ matrices G_μ which either have a unit element somewhere in the main diagonal and zeros everywhere else or have a unit element somewhere above the main diagonal, its mirror image below, and zeros everywhere else. The set $\{G_\mu\}$ forms a complete basis for real and symmetric matrices. In contradistinction, the matrices $C_{\mu\nu}(J,\alpha)$ do not form such a complete set. To be sure, every matrix $C_{\mu\nu}(J,\alpha)$ may be thought of as a linear combination of the G_μ. But the number of matrices $C_{\mu\nu}(J,\alpha)$ is typically much smaller than $N(N+1)/2$. Therefore, many other linear combinations of the G_μ exist which are linearly independent of $C_{\mu\nu}(J,\alpha)$ and which do not occur in the TBRE. The TBRE may be negatively defined by constraining all such linear combinations to be zero.

We present evidence that the matrices $C_{\mu\nu}(J,\alpha)$ are the agents which cause chaos in the TBRE. In anticipation of this result, we give a qualitative argument why every matrix $C_{\mu\nu}(J,\alpha)$ may be thought of as a single representation of the GOE. In constructing the many-body basis states $|J\mu\rangle$, we may proceed as follows. We form Slater determinants by distributing m nucleons over the single-particle states of a major shell. These are antisymmetric by construction but do not possess good quantum numbers J. States with good J are obtained as linear combinations of such Slater determinants, a typical state $|J\mu\rangle$ consisting of a linear combination of *many* determinants. Although the two-body interaction has nonvanishing matrix elements only between determinants that differ in the occupation numbers of not more than two single-particle states, that fact makes sure that the matrices $C_{\mu\nu}(J,\alpha)$ are densely filled. Moreover, the coefficients in the linear combinations are determined by angular momentum algebra, i.e., contain Clebsch-Gordan coefficients, Racah coefficients, and coefficients of fractional parentage. Although individually determined group theoretically, these quantities combine to make the coefficients of the linear combinations almost random numbers. This stochastic aspect of the shell model has been emphasized by Zelevinsky *et al.* (1996) who employed the term "geometric chaoticity."

Thus, the matrices $C_{\mu\nu}(J,\alpha)$ are dense and their elements are close to being random. Our qualitative argument is subject to two caveats. First, the dimension of the matrices $C_{\mu\nu}(J,\alpha)$ is always finite. Second, the matrices $C_{\mu\nu}(J,\alpha)$ are not dense everywhere and may have a substructure with blocks that are completely empty. Consider, for instance, the sd shell and the two-body operator α_0 which scatters a pair of nucleons in states $(d_{3/2},d_{3/2})$ into states $(d_{5/2},d_{5/2})$. The two-body operator has vanishing matrix elements between all many-body states $|J\mu\rangle$ which are constructed by filling only the $s_{1/2}$ and $d_{3/2}$ shells with m nucleons. The same statement applies to the matrix $C_{\mu\nu}(J,\alpha_0)$.

III. PROPERTIES OF THE TBRE

In this section we present several properties of the TBRE which are either fundamentally different from those of the GOE or have no counterpart in the latter. The material in this section is largely taken from Papenbrock and Weidenmüller (2004, 2005, 2006). The numerical examples are all obtained in the *sd* shell or in a single *j* shell.

A. How the matrices $C_{\mu\nu}(J,\alpha)$ mix the states

The *sd* shell has subshells $s_{1/2}$, $d_{5/2}$, and $d_{3/2}$. Let n_i with $i=1,2,3$ denote the occupation numbers of these three subshells and $m=\Sigma_i n_i$ the total number of nucleons in the *sd* shell. The many-body basis states $|J\mu\rangle$ can be ordered in blocks with fixed values of $\{n_1,n_2,n_3\}$. For $m=12$ there exist 41 such partitions. The two-body matrix elements $v(\alpha)$ belong to one of three classes: (i) They leave the partition unchanged so that $\{n_1,n_2,n_3\} \rightarrow \{n_1,n_2,n_3\}$ (28 two-body matrix elements); (ii) they change the partition by moving one nucleon from one subshell to another while leaving the second nucleon in its subshell so that $\{n_1,n_2,n_3\}\rightarrow\{n_1+1,n_2-1,n_3\}$, etc. (22 two-body matrix elements); or (iii) they change the partition by moving both nucleons from one subshell to another so that $\{n_1,n_2,n_3\}\rightarrow\{n_1-1,n_2-1,n_3+2\}$ cyclic or to $\{n_1-2,n_2+1,n_3+1\}$ cyclic (13 two-body matrix elements). The same classification applies to the matrices $C_{\mu\nu}(J,\alpha)$ since each of these and the corresponding $v(\alpha)$ contain the same two-body operator. Therefore, the $C_{\mu\nu}(J,\alpha)$ acquire block structure. For 12 nucleons coupled to $J=0$, $T=0$ this is shown in Fig. 13 where the 839 states are ordered according to the sizes of the blocks to which they belong.

The block structure is clearly a consequence of the shell model with its subshells. It is bound to occur in every major shell. The structure is completely absent in the GOE where the matrices are densely filled. It is clear that a single matrix $C_{\mu\nu}(J,\alpha)$ cannot mix the states completely. Such mixing can be accomplished only by a linear combination of most or all of $C_{\mu\nu}(J,\alpha)$ as in Eq. (6). Put differently, it is clear that a single or a few nonvanishing matrix elements $v(\alpha)$ cannot lead to a complete mixing of the basis states, i.e., to chaos. We expect that we need most or all of $v(\alpha)$ for that purpose. This observation illustrates the caveat "with the exception of a set of measure zero" presented in Sec. II.B: Putting one or several $v(\alpha)$'s identically equal to zero reduces the set $\{v(\alpha)\}$ to a set of measure zero with respect to the integration over all variables $v(\alpha)$. The observation also sheds light on and reinforces the concept geometric chaoticity (Zelevinsky *et al.*, 1996). Indeed, the mixing is both made possible and limited by geometric constraints that result from the coupling of single-particle states to many-body states with good quantum numbers.

A few numbers may illustrate the way in which the matrices $C_{\mu\nu}(J,\alpha)$ fill their individual blocks. As a measure for such filling, we use the number of $C_{\mu\nu}(J,\alpha)$
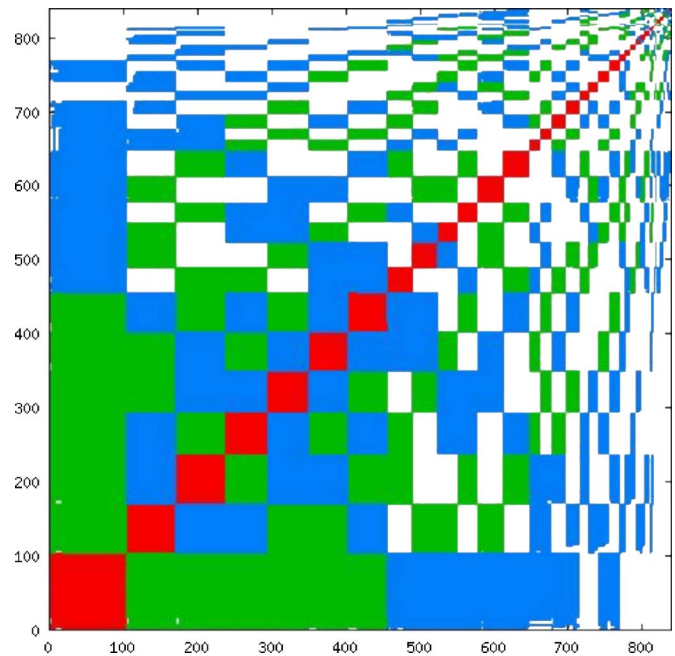

FIG. 13. (Color online) The block structure of the matrices $C_{\mu\nu}(J,\alpha)$ for $m=12$ nucleons in the *sd* shell coupled to total spin $J=0$ and total isospin $T=0$. Black (color online: red), no change of partition. Light gray (color online: green), change of partition by moving one nucleon. Dark gray (color online: blue), change of partition by moving two nucleons. White: there is no two-body matrix element that connects the states in question. From Papenbrock and Weidenmüller, 2005.

which contribute on average to a given matrix element. When the partition is not changed [black (color online: red) blocks in Fig. 13], that number is 25.2 ± 4.0 (out of a total of 28 matrices). Within the black blocks, mixing is thus very thorough. This statement is supported by another measure (inverse participation ratios) not shown here. For the light gray (color online: green) blocks, the corresponding number is 7.2 ± 1.4 (out of a total of 22 matrices) and for the dark gray (color online: blue) blocks, 2.0 ± 0.9 (out of a total of 13 matrices). Similar values are obtained in the case of a single *j* shell. The wealth of available numerical data (see, for instance, Figs. 11 and 12) shows that there is chaos for some choices of $v(\alpha)$. This is not an accidental feature related to a particular choice of the residual interaction. Indeed, the numbers given show that the mixing of states within each of the diagonal (red) blocks is virtually complete for almost every choice of the residual interaction. This fact ensures that a few nondiagonal matrix elements suffice to also mix different diagonal blocks very efficiently with each other. Thus, the seemingly small numbers cited for the light and dark gray blocks are actually quite sufficient to accomplish complete mixing of all states, even though some (white) blocks carry zero entries. As a result, we conclude from the structure of the matrices $C_{\mu\nu}(J,\alpha)$ that chaos is a generic structural property of the *sd* shell. Since other major shells are structurally similar to the *sd* shell, we conclude that chaos is generic in the shell model at large. We formulate this statement

with one proviso: We have neglected the differences in the single-particle energies pertaining to different subshells. In realistic cases, our statement applies only if the magnitude of the matrix elements of the residual interaction is sufficiently large to strongly mix different subshells. This is the case in practice.

While different subshells are mixed quite thoroughly and chaos is expected to prevail within every major shell, different major shells do largely retain their identity because the magnitudes of $v(\alpha)$ are typically small compared to the spacings of major shells. This is demonstrated by experimental facts on the behavior of the neutron strength function or of spectroscopic factors which unfortunately cannot be presented and explained in the present framework (Lapikas, 1993).

We reiterate the remark that strong mixing within a major shell does not preclude the existence of individual states at higher excitation energies that can be identified as distinct modes of motion of the nucleus (like the giant-dipole resonances). Deformed nuclei display collective motion like rotational bands and, in the ground-state domain, deviations from Wigner-Dyson spectral fluctuations. This last fact has been extensively discussed in the literature [see Abul-Magd *et al.* (2004), and references to earlier work therein]. At this point, it is not clear how such features can be reconciled with the view of chaos in nuclei presented in this paper.

B. Information content of nuclear spectra

The GOE spectra do not carry any information content. Spectral fluctuations in nuclei often agree with GOE predictions. Are such spectra void of physical information? We answer this question in quantitative terms (Papenbrock and Weidenmüller, 2006) but begin with a qualitative consideration.

The Hamiltonian (6) contains the matrix elements $v(\alpha)$ as parameters and is otherwise fixed. The number of these parameters is typically small compared with the matrix dimension. Therefore, a small number of data points (for instance, energies of levels with fixed spin J) suffices, in principle, to determine $H_{\mu\nu}(J)$. The Hamiltonian matrices of the levels with spins $J' \neq J$ are governed by the *same* set of matrix elements $v(\alpha)$ [only the matrices $C_{\mu\nu}(J', \alpha)$ differ in form and dimension] and are, therefore, also known once the $v(\alpha)$ are determined. Hamiltonians describing other nuclei (different mass numbers) pertaining to the same major shell are likewise governed by the set $\{v(\alpha)\}$ and, thus, known too. [Again a caveat is needed: The set $\{v(\alpha)\}$ which empirically describes the data best may change with mass number.] Thus, the situation is radically different from that of the GOE because the matrices $C_{\mu\nu}(J, \alpha)$ (the agents of chaos) are fixed by the shell model. A small number of parameters determines spectra of many J values in many nuclei. TBRE spectra do carry information.

We now turn to the quantitative question: How reliably can this information be deduced from the data? To this end we cast the Hamiltonian (6) in another form.

We seek a decomposition of the Hamiltonian into a sum of matrices that can be ordered with respect to their relevance or importance. The decomposition (6) is not useful for this purpose: The matrices $C_{\mu\nu}(J, \alpha)$ exhibit some degree of linear independence but a stronger metric concept is called for. For this purpose, we introduce the canonical scalar product for matrices and switch from the matrices $C_{\mu\nu}(J, \alpha)$ to new matrices $B_{\mu\nu}(J, \alpha)$ that form an orthonormal basis set. With $d(J)$ the dimension of the Hilbert space spanned by the state vectors $|J\mu\rangle$, we define the real and symmetric overlap matrices

$$S_{\alpha\beta}(J) = d^{-1}(J)\mathrm{Tr}[C(J, \alpha)C(J, \beta)]. \tag{7}$$

These are diagonalized by orthogonal transformations $\mathcal{O}(J)$,

$$\{\mathcal{O}(J)S(J)[\mathcal{O}(J)]^T\}_{\alpha\beta} = s_\alpha^2(J)\delta_{\alpha\beta}, \tag{8}$$

where T denotes the transpose. The matrices $S_{\alpha\beta}(J)$ are positive semidefinite so that $s_\alpha^2(J) \geq 0$. The eigenvalues are arranged by decreasing magnitude, $s_1^2(J) \geq s_2^2(J) \geq \cdots \geq 0$. The real roots $s_\alpha(J)$ of $s_\alpha^2(J)$'s are chosen positive or zero. If one or several eigenvalues vanish, we conclude from Eqs. (8) and (7) that there exist one or several linear combinations of the matrices $C(J, \alpha)$ that vanish identically. For the $a_1(J)$ nonvanishing eigenvalues $s_\alpha^2(J)$, we define

$$B_{\mu\nu}(J, \alpha) = \frac{1}{s_\alpha(J)}\sum_\beta \mathcal{O}_{\alpha\beta}C_{\mu\nu}(J, \beta), \quad \alpha = 1, \ldots, a_1(J). \tag{9}$$

Except for possible degeneracies among the eigenvalues $s_\alpha^2(J)$, the matrices $B_{\mu\nu}(J, \alpha)$ are defined uniquely. By construction, these matrices are orthonormal with respect to the trace,

$$d^{-1}(J)\mathrm{Tr}[B(J, \alpha)B(J, \beta)] = \delta_{\alpha\beta}. \tag{10}$$

Written in terms of the matrices $B(J, \alpha)$, the Hamiltonian takes the form

$$H_{\mu\nu}(J) = \sum_{\alpha=1}^{a_1} w(J, \alpha)s_\alpha(J)B_{\mu\nu}(J, \alpha). \tag{11}$$

We note that the eigenvalues $s_\alpha^2(J)$ indicate the weight and relevance of the corresponding basis matrix $B(J, \alpha)$ in the construction of the Hamiltonian (11). This weight has purely geometric origin. The dynamical weight $w(J, \alpha)$ stems from the two-body interaction and is given by

$$w(J, \alpha) = \sum_\beta \mathcal{O}_{\alpha\beta}v(\beta), \quad \alpha = 1, 2, \ldots, a_1. \tag{12}$$

The $w(J, \alpha)$ have the same distribution as $v(\alpha)$: They are Gaussian-distributed random variables with mean values zero and a common second moment. The form of the Hamiltonian (11) with the definitions (9) and (12) is completely equivalent to the original expression (6). It allows us to quantify the information content of nuclear spectra. If for some value of J one or several eigenvalues
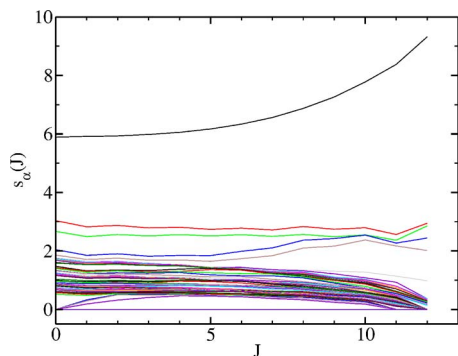
FIG. 14. (Color online) Roots $s_\alpha(J)$ of the eigenvalues $s_\alpha^2(J)$ defined in Eq. (8) vs total spin J for the $T=0$ states in ^{24}Mg. From Papenbrock and Weidenmüller, 2006.

$s_\alpha^2(J)$ vanish, the number $a_1(J)$ of variables $w(J,\alpha)$ is smaller than the number of elements $v(\alpha)$. For such a value of J it is then impossible to determine more than $a_1(J)$ linear combinations of the $v(\alpha)$ from the data. We show below that such vanishing eigenvalues always occur. Moreover, if some eigenvalues are significantly smaller than the leading ones, then Eq. (11) shows that their influence on the spectrum is small [we recall that the matrices $B(J,\alpha)$ obey Eq. (10)] and it will be difficult to deduce their values from the data. We conclude that it is important to determine the eigenvalues $s_\alpha^2(J)$. The determination can be done without prior knowledge of the form of the residual interaction [i.e., of the values of the $v(\alpha)$] since the eigenvalues are determined by the matrices $C_{\mu\nu}(J,\alpha)$, i.e., by the shell model itself.

Papenbrock and Weidenmüller (2005, 2006) gave the distribution of the roots $s_\alpha(J)$ of the eigenvalues for a single j shell with $j=19/2$ and for some nuclei in the sd shell. All these distributions are very similar. By way of example, we reproduce in Fig. 14 the graph for the states with isospin 0 in the nucleus ^{24}Mg.

We note that all roots change smoothly with J. The largest $s_1(J)$ is significantly larger than all others. For the case of the single j shell, it can be shown analytically that the corresponding linear combination $B_{\mu\nu}(J,1)$ of the matrices $C_{\mu\nu}(J,\alpha)$ is approximately equal to the matrix representation of the monopole operator which in turn is approximately equal to the unit matrix. The numerical results indicate that these statements are generic; they hold also for ^{24}Mg. Hence, $s_1(J)$ determines essentially the centroid of the spectrum of states with spin J and has little influence on spectral fluctuations. The latter are largely determined by the remaining nonvanishing eigenvalues and associated matrices $B_{\mu\nu}(J,\alpha)$. Because of the orthogonality relation (10), the latter are almost traceless.

The root $s_1(J)$ is followed in magnitude by four eigenvalues that are distinct from the remaining set. We observe that some eigenvalues in that set vanish for large values of J (this is because the matrix dimension shrinks with increasing J and eventually becomes too small to support a large number of eigenvalues) and that at least

one eigenvalue vanishes for all values of J. This is because the operator $\vec{J}^2$ for total spin J is a two-body operator. Thus, the matrix representation of the term $\vec{J}^2 -J(J+1)$ can be written as a linear combination of the matrices $C_{\mu\nu}(J,\alpha)$. This linear combination vanishes identically.

Figure 14 shows that it is difficult to determine those $w(J,\alpha)$'s from data which belong to the smallest eigenvalues and that the problem cannot be solved by combining data for different spin values. Practitioners of the shell model avoid the difficulty by combining a fit to data with *ab initio* values of $v(\alpha)$ obtained from many-body theory; see, for instance, Brown and Wildenthal (1988) and Honma *et al.* (2004).

C. Preponderance of ground states with spin zero

Johnson *et al.* (1998) reported that in even-even nuclei (nuclei with even proton and neutron numbers), the TBRE yields ground states with spin zero much more frequently than corresponds to the fraction of spin-zero states in the model space. Subsequent work by Bijker and Frank (2000) and by Jaquod and Stone (2000) showed that similar regularities exist in bosonic and electronic many-body systems, respectively. The phenomenon has received intense attention, and we refer the reader to the reviews by Zelevinsky and Volya (2004) and Zhao *et al.* (2004). The problem has been understood quantitatively for bosonic models of the nucleus within mean-field calculations (Bijker and Frank, 2001). For the nuclear shell model, two approaches yield good agreement with numerical simulations. Zhao *et al.* (2002) devised an algorithm that accurately predicts the fraction of ground states with a given spin. The other approach considers fluctuations and correlations between the J-dependent spectral widths and also leads to semiquantitative predictions. This approach was put forward by Papenbrock and Weidenmüller (2004) and is described in what follows.

The key to understanding the phenomenon is the observation that the spectral widths σ_J of states with different J values are correlated. The spectral widths are defined by

$$\sigma_J^2 = d^{-1}(J)\mathrm{Tr}[H^2(J)]. \tag{13}$$

From Eqs. (11) and (10), we have

$$\sigma_J^2 = \sum_{\alpha=1}^{a_1} w^2(J,\alpha)s_\alpha^2(J). \tag{14}$$

Spectral widths pertaining to different J depend upon the same random variables $v(\alpha)$ [the $w(J,\alpha)$ are linear functions of the $v(\alpha)$; see Eq. (12)] and are, therefore, correlated.

Before using this fact, we relate the spectral width σ_J to the position of the lowest (or highest) state with spin J—more precisely, to the distance R_J of the lowest (or highest) level in the spectrum from the origin (the spectral radius). [We do not distinguish the lowest from the
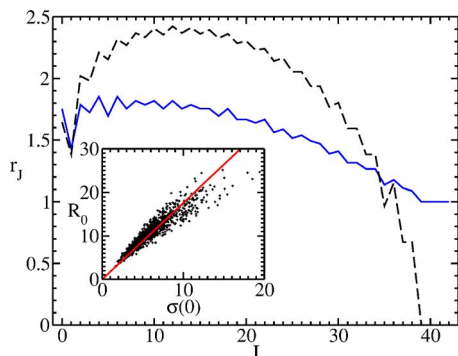
FIG. 15. (Color online) The scaling factor r_J of Eq. (13) versus J for six fermions in the $j=19/2$ shell (solid line). Inset: Linear fit to r_J for the states with $J=0$. The dots correspond to 900 realizations of the ensemble. From Papenbrock and Weidenmüller, 2004.

FIG. 16. (Color online) Six fermions in the $j=19/2$ shell with 900 realizations of the TBRE. Solid line: Numerical probabilities for σ_J to have maximum value. Dashed line: Numerical probabilities for $r_J\sigma_J$ to have maximum value. Dots: Numerical probabilities for state with spin J to be the ground state. From Papenbrock and Weidenmüller, 2004.

highest state since the $v(\alpha)$ have random signs.] The spectral radius is expected to be a random variable. We ask for the probability p_j with which, for a given value of J, R_J takes maximum value. The probability of finding a ground state with spin J is given by p_J.

We define the scaling factor r_J by writing

$$R_J = r_J\sigma_J. \tag{15}$$

Equation (15) is useful in the present context because it turns out that (in contrast to σ_J) r_J hardly fluctuates with $v(\alpha)$. For the case of six fermions in the $j=19/2$ shell and for the states with spin $J=0$, this is shown in the inset of Fig. 15. Similarly constant (nonfluctuating) behavior of r_J was found for other cases (different spin values, different number of nucleons, and nuclei in the sd shell). Therefore, the fluctuations and correlations of the widths σ_J directly affect those of the spectral radii R_J. The linear fits to r_J, obtained as shown in the inset, are used for the plot of r_J versus J shown in Fig. 15 (and similarly for other cases). The overall monotonic decrease of r_J with J reflects the overall monotonic decrease of the dimensions $d(J)$ with J. Indeed, average shell-model spectra are known to have approximately Gaussian shape. It is then intuitively obvious that r_J grows with $d(J)$. The decrease of r_J with increasing J shown in Fig. 15 enhances the chance for states with small spins J to form the ground state. The same is true for the odd-even staggering of r_J (which is due to the same reason and gives, for instance, preference to spin zero over spin 1).

It remains to study the probabilities that the spectral widths σ_J attain maximum values. For the case displayed in Fig. 15, these are shown as solid lines in Fig. 16. The states with lowest and highest spins have the largest probabilities. Here correlations play a role: For some choice of $v(\alpha)$, the spectral width for some other spin value may take an unusually large value but so do, at the same time and for most cases, σ_0 and σ_{42}. The dashed line in Fig. 16 gives the probability that the product $r_J\sigma_J$ attains maximum value. Because of the effect shown in Fig. 15, the highest spin value is suppressed and spin 0
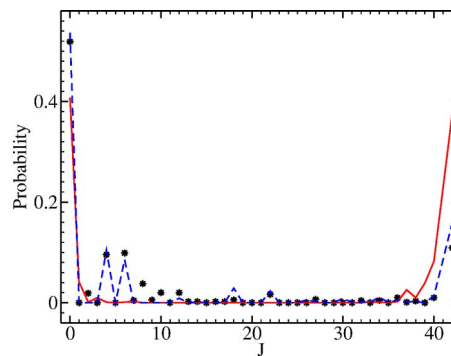
wins. The result must be compared with the actual probabilities (dots) that a state with spin J forms the ground state. The agreement, although not perfect, shows that the explanation accounts for the main features of the phenomenon.

Similar results were obtained for eight fermions in the $j=19/2$ shell for ^{20}Ne and for ^{24}Mg. Figure 17 shows the case of states with $T=0$ in ^{24}Mg.

D. Correlations between spectra carrying different quantum numbers

In the TBRE the preponderance of ground states with spin zero is, to a large extent, due to correlations between spectral widths σ_J pertaining to different values of J. The correlations are caused by the fact that all widths σ_J depend on the same random variables $v(\alpha)$. Equation (6) shows that the same statement holds for the Hamiltonians $H_{\mu\nu}(J)$ pertaining to different spin values and, more generally, for the Hamiltonians pertaining to nuclei belonging to the same major shell.

From the point of view of the shell model, these statements are not terribly surprising. A change of the residual interaction causes simultaneous changes in the spectra of all nuclei belonging to the same major shell.
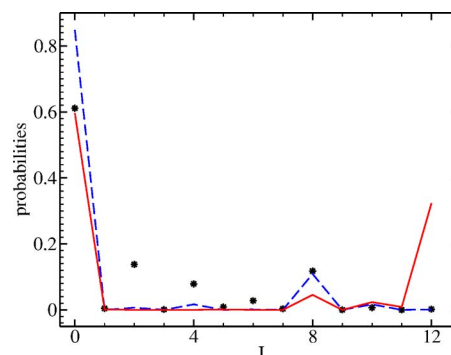

FIG. 17. (Color online) Same as Fig. 16 for the $T=0$ states in ^{24}Mg. From Papenbrock and Weidenmüller, 2006.

In the framework of a statistical description, this fact is tantamount to the existence of spectral correlations. Still, it is remarkable that such correlations have never been addressed in the framework of RMT until quite recently. It is, in fact, not obvious how to model such correlations in canonical RMT. The standard approach consists of assuming that correlations do not exist. This assumption is usually stated explicitly in the statistical theory of nuclear reactions. Let $S_{ab}(E,J)$ be an element of the statistical scattering matrix for scattering from channel a into channel b at energy E and total spin J. It is assumed that elements pertaining to different J values are uncorrelated. This assumption implies the symmetry of compound-nucleus scattering cross sections about 90° scattering angle in the center-of-mass system.

It is of interest to test these standard assumptions of RMT using the TBRE. While tests for correlations of the statistical scattering matrix have apparently not yet been performed, tests of spectral correlations for levels both in the same nucleus carrying different quantum numbers and in different nuclei do exist (Papenbrock and Weidenmüller, 2006). The level density $\rho(E,J)$ for levels with spin J and energies $E_\mu(J)$ (where μ is a running index) is given by

$$\rho(E,J) = \sum_\mu \delta(E - E_\mu(J)). \tag{16}$$

As a measure of spectral correlations, we use the correlator

$$C(E_1,J_1;E_2,J_2) = \overline{\rho(E_1,J_1)\rho(E_2,J_2)} - \overline{\rho(E_1,J_1)}\,\overline{\rho(E_2,J_2)}. \tag{17}$$

In Fig. 18 we show the two terms on the right-hand side of Eq. (17) and the resulting correlator versus the energies E_1 and E_2 of the two sets of spin states for the $J=0$, $T=0$ and the $J=2$, $T=0$ states in ^{24}Mg. The correlator has a maximum value of about 13% of the mean value of the product of the level densities.

In Fig. 19 we show the same quantities for the $J=0$, $T=0$ states in ^{22}Ne and ^{24}Mg. Here the correlator has a maximum value of 6%. In both cases, the existence of spectral correlations is firmly established.

The correlators shown in Figs. 18 and 19 are obtained by averaging over the ensemble and are, therefore, entirely theoretical. Do they have any correspondence in reality (where we deal with a single Hamiltonian rather than an ensemble)? Presently, this question cannot be answered using experimental data—the data set is not sufficient. However, shell-model calculations can serve as a substitute. Realistic single-particle energies and an optimized two-body interaction (Brown and Wildenthal, 1988) were used to calculate the energies of low-lying states with spins $J=0$ and 2 ($J=1/2$ and $5/2$) in a number of even-even (odd-even, respectively) nuclei in the sd shell (Papenbrock and Weidenmüller, 2006). The correlations between nearest-neighbor level spacings of the lowest few states with different spins were evaluated as in Eq. (17), the ensemble average being replaced by the running average over the set of nuclei just mentioned.
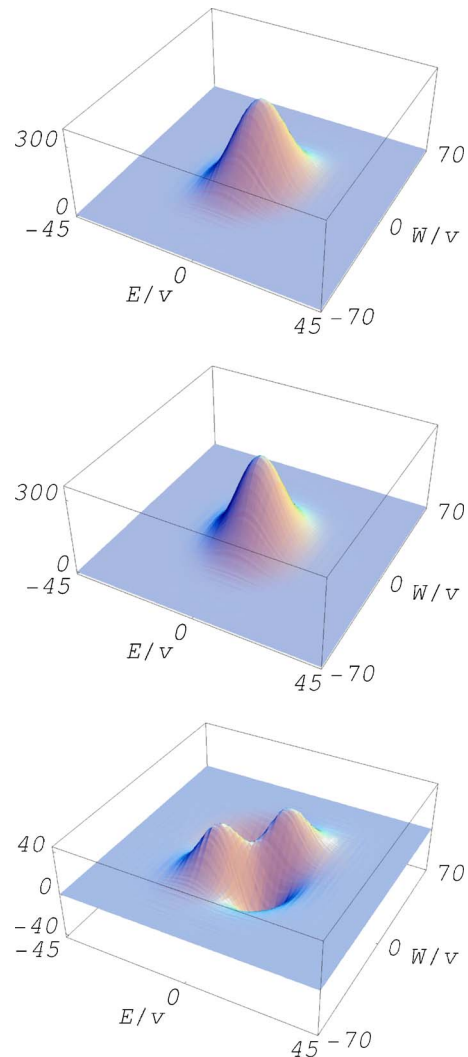

FIG. 18. (Color online) Correlations between the level densities for states with spin 0 and spin 2 (both with $T=0$) in ^{24}Mg. Left panel: Mean value of the product of the two level densities. Middle panel: Product of the mean level densities. Right panel: The correlator of Eq. (17) (from 400 realizations of the ensemble). From Papenbrock and Weidenmüller, 2006.

Figure 20 shows the result (displayed in the same form as in Figs. 18 and 19). Again, the existence of correlations is established. We observe that these are particularly pronounced for the lowest levels where they amount to about 10%.

Our analysis establishes the existence of correlations between spectra carrying different quantum numbers. All examples were taken from the sd shell, however, where the dimensions of the Hamiltonian matrices are rather small (typically 10^2–10^3). The maxima of the correlators are in the 10% range. It is not clear how these results carry over to other major shells where both the matrix dimensions and the number of independent two-body matrix elements are much larger. The statistical theory of nuclear reactions is mainly used in such shells. Therefore, definitive conclusions must wait for further analysis.
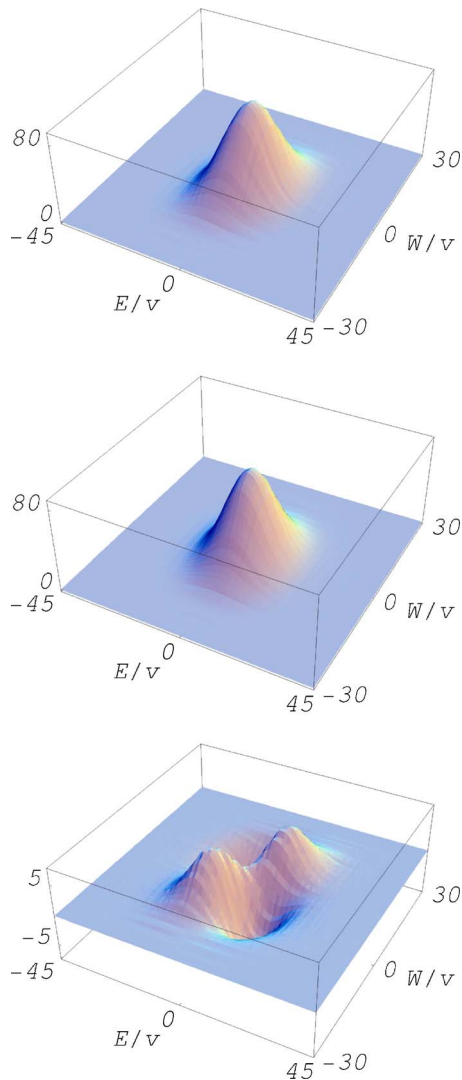
FIG. 19. (Color online) Same as Fig. 18 except for the correlations between the level densities for states with spin 0 and isospin 0 in ^{20}Ne and in ^{24}Mg. Left panel: Mean value of the product of the two level densities. Middle panel: Product of the mean level densities. Right panel: The correlator of Eq. (17) (from 400 realizations of the ensemble). From Papenbrock and Weidenmüller, 2006.
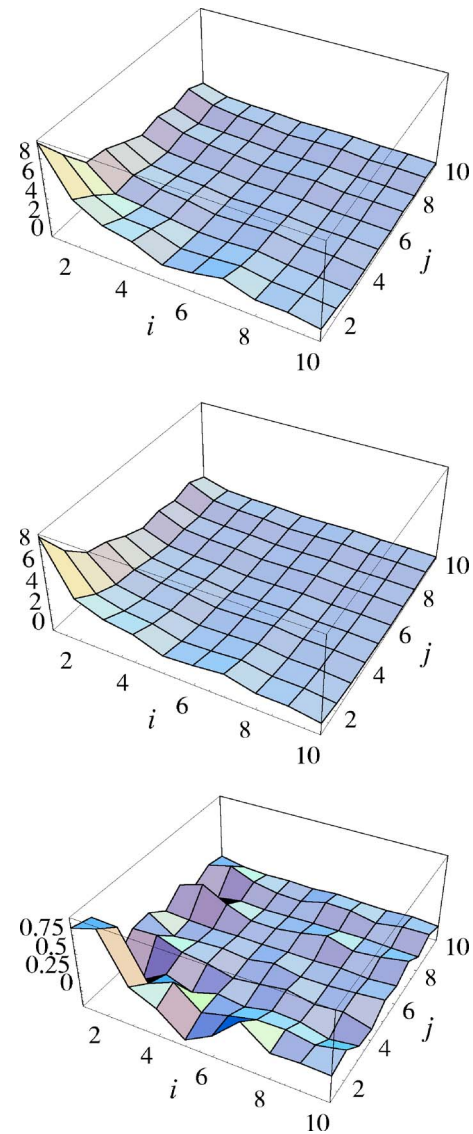

FIG. 20. (Color online) Same as Fig. 18 except for the correlations between pairs of nearest-neighbor spacings of low-lying levels with different spins obtained by averaging over a number of nuclei in the *sd* shell (see text). The indices *i* and *j* label the spacings consecutively starting from the lowest state. Left panel: Mean value of the product of the two spacings. Middle panel: Product of the mean values of the two spacings. Right panel: The correlator. From Papenbrock and Weidenmüller, 2006.

IV. SUMMARY AND CONCLUSIONS

In the first part of this paper, we introduced random matrices and the concept of (quantum) chaos. Both are linked by the Bohigas-Giannoni-Schmit conjecture. Random-matrix theory predicts fluctuation properties of spectra in a parameter-free fashion. In many cases, the fluctuation properties of nuclear spectra agree with these predictions: The nuclear dynamics is (partly) chaotic. To relate this observation to known dynamical features of spherical nuclei, we described, in the second part, the nuclear shell model (a mean-field theory with residual interactions). We pointed out that shell-model spectra also show chaos. To explain this observation, we defined the two-body random ensemble as the generic Gaussian random-matrix ensemble of the shell model.

In the third part, we displayed a number of properties of that ensemble, mainly using the *sd* shell. We focused attention on those properties in which the TBRE differs from standard RMT: (i) The TBRE generically produces chaos. Thus, chaos in nuclei is not due to a particular feature of the residual interaction. The mechanism which mixes the basis states of Hilbert space differs significantly from that of canonical RMT. Chaos is due to the building block matrices $C_{\mu\nu}(J, \alpha)$. In each major shell, these matrices are fixed once and for all. They are determined entirely by intrinsic properties of the shell model and are independent of any particular residual interaction. (ii) The spectra of matrices drawn at random

from a canonical ensemble of RMT do not carry any information content. Because of the role played by the fixed matrices $C_{\mu\nu}(J, \alpha)$, this is not so for the TBRE. On the contrary, it is possible to extract relevant physical information from nuclear spectra. We have analyzed the degree to which this can be done. (iii) The preponderance of ground states with spin zero in the TBRE is, to a large extent, due to correlations between widths of spectra with different spin values. (iv) Correlations exist more generally also between spectra carrying different quantum numbers and in different nuclei belonging to the same major shell. The implications of this last statement have not yet been fully explored.

The examples used to illustrate or prove these assertions were taken from the *sd* shell or from a single *j* shell. The line of reasoning strongly suggests, however, that the spectral fluctuation properties of the TBRE agree with RMT predictions for all major shells. We confined ourselves to a two-body residual interaction and to the TBRE. It is obvious that the inclusion of three-body forces would enhance the tendency of the system towards chaotic dynamics.

Throughout most of the paper, we assumed that the single-particle energies of subshells belonging to a major shell are degenerate. Within this approximation, we have shown that quantum chaos is a generic feature of the nuclear shell model. This means that most choices of the residual interaction will result in spectra showing spectral fluctuations that agree with RMT predictions. Actually, the neglect of the differences of single-particle energies of subshells is not completely justified. The magnitude of a typical two-body matrix element which mixes different subshells is comparable with the difference of the corresponding single-particle energies. The resulting incomplete mixing of many-body states within a major shell reveals itself in slight deviations from RMT predictions (Zelevinsky *et al.*, 1996). Moreover, the residual interaction is far too weak to thoroughly mix adjacent major shells. This is why shell structure remains the hallmark of nuclear physics, in spite of quantum chaos. It is in that sense that spherical nuclei display only partial quantum chaos.

Low-lying states in spherical nuclei often display regular features. This statement is not at variance with our conclusions. Indeed, chaos manifests itself mainly in the fluctuation properties of spectra. These are defined in terms of statistical measure tests of which require a large number of levels with identical quantum numbers. The regular features refer to the properties of a small number of levels in the ground-state domain which carry different quantum numbers. The properties of these levels may be particularly sensitive to a specific component of the two-body interaction. Modeling the entire residual interaction in terms of these components may give rise to regular motion.

Our discussion has been confined to spherical nuclei. Nuclei with mass numbers lying in the middle of large major shells (like the rare-earth nuclei) cannot be successfully described in terms of the spherical shell model. The dimensions of the many-body Hilbert spaces are too large. One uses instead collective models with a small number of degrees of freedom. The connection between these and the spherical shell model is not firmly established. However, quantum chaos is prevalent in these nuclei, too, with the exception of cases of distinct symmetries (Alhassid and Whelan, 1991).

There are several open questions and directions for future research. (i) We are still lacking a deeper analytical understanding of the TBRE and its fluctuation properties. An analytical approach must be based on properties of the matrices denoted here by $C_{\mu\nu}(J, \alpha)$. While a theoretical description for shells with several subshells is probably difficult, focusing on a single *j* shell might simplify the problem. (ii) The TBRE predicts correlations between spectra with different quantum numbers (e.g., different masses, spins, or isospins) for nuclei within a major shell. Experimental verification is difficult due to limitations in the length and completeness of observed nuclear spectra, but other Fermi systems might be more accessible. (iii) The correlations between spectra with different quantum numbers might also affect the scattering matrix, more precisely, such correlations might induce correlations among *S*-matrix elements carrying different total spin quantum numbers. The present analysis of fluctuating cross sections in compound nuclei neglects any such correlations. A better understanding of this problem would be highly desirable.

Nuclear spectroscopy is a mature field with a history of more than 50 years. In spite of this fact it continues to offer great challenges. We have addressed one of them: the way chaos is induced by the two-body interaction of the shell model, an interaction which is at the same time responsible for the many regular features seen in nuclei.

ACKNOWLEDGMENTS

REFERENCES

Abul-Magd, A. Y., H. L. Harney, M. H. Simbel, and H. A. Weidenmüller, 2004, Phys. Lett. B **579**, 278.

Ajzenberg-Selove, J., 1987, Nucl. Phys. A **475**, 1.

Alhassid, Y., and N. Whelan, 1991, Phys. Rev. Lett. **67**, 816.

Benet, L., and H. A. Weidenmüller, 2003, J. Phys. A **36**, 3569.

Bijker, R., and A. Frank, 2000, Phys. Rev. Lett. **84**, 420.

Bijker, R., and A. Frank, 2001, Phys. Rev. C **64**, 061303.

Bohigas, O., and J. Flores, 1971, Phys. Lett. **34B**, 261.

Bohigas, O., E. M. Giannoni, and C. Schmit, 1986, Phys. Rev. Lett. **52**, 1.

Bohr, A., and B. Mottelson, 1975, *Nuclear Structure* (Benjamin, New York), Vol. II.

Bohr, N., 1936, Nature (London) **137**, 344.

Brown, B. A., and B. H. Wildenthal, 1988, Annu. Rev. Nucl.

Part. Sci. **38**, 29.

Dyson, F. J., 1962a, J. Math. Phys. **3**, 140.

Dyson, F. J., 1962b, J. Math. Phys. **3**, 157.

Dyson, F. J., 1962c, J. Math. Phys. **3**, 1199.

French, J. B., and S. S. M. Wong, 1970, Phys. Lett. **33B**, 449.

Garg, J. B., J. Rainwater, J. S. Petersen, and W. W. Havens, Jr., 1964, Phys. Rev. **134**, B985.

Guhr, T., A. Müller-Groeling, and H. A. Weidenmüller, 1998, Phys. Rep. **299**, 189.

Haake, F., 2001, *Quantum Signatures of Chaos*, 2nd enlarged ed. (Springer-Verlag, Berlin).

Haq, R. V., A. Pandey, and O. Bohigas, 1982, Phys. Rev. Lett. **48**, 1086.

Haq, R. V., A. Pandey, and O. Bohigas, 1983, in *Nuclear Data for Science and Technology*, edited by K. H. Böckhoff (Reidel, Dordrecht), p. 209.

Heusler, S., S. Müller, A. Altland, P. Braun, and F. Haake, 2007, Phys. Rev. Lett. **98**, 044103.

Honma, M., T. Otsuka, B. A. Brown, and T. Mizusaki, 2004, Phys. Rev. C **69**, 034335.

Jaquod, P., and A. D. Stone, 2000, Phys. Rev. Lett. **84**, 3938.

Johnson, C. W., G. F. Bertsch, and D. J. Dean, 1998, Phys. Rev. Lett. **80**, 2749.

Kota, V. B. K., 2001, Phys. Rep. **347**, 223.

Lane, T., and R. Thomas, 1958, Rev. Mod. Phys. **30**, 257.

Lapikas, L., 1993, Nucl. Phys. A **553**, 297c.

Mayer, M., and J. H. D. Jensen, 1955, *Elementary Theory of Nuclear Shell Structure* (Wiley, New York).

Mehta, M. L., 2004, *Random Matrices*, 3rd ed. (Academic, New York).

Mon, K. K., and J. B. French, 1975, Ann. Phys. (N.Y.) **95**, 90.

Papenbrock, T., and H. A. Weidenmüller, 2004, Phys. Rev. Lett. **93**, 132503.

Papenbrock, T., and H. A. Weidenmüller, 2005, Nucl. Phys. A **757**, 422.

Papenbrock, T., and H. A. Weidenmüller, 2006, Phys. Rev. C **73**, 014311.

Porter, C. E., 1965, *Statistical Theories of Spectra: Fluctuations* (Academic, New York).

Wigner, E. P., 1955, Ann. Math. **62**, 548.

Wigner, E. P., 1959, Report No. ORNL-2309, Oak Ridge National Laboratory (reprinted in Porter, 1965), p. 188.

Zelevinsky, V., B. A. Brown, N. Frazier, and M. Horoi, 1996, Phys. Rep. **276**, 85.

Zelevinsky, V., and A. Volya, 2004, Phys. Rep. **391**, 311.

Zhao, Y. M., A. Arima, and N. Yoshinaga, 2002, Phys. Rev. C **66**, 034302.

Zhao, Y. M., A. Arima, and N. Yoshinaga, 2004, Phys. Rep. **400**, 1.